tvst

Retina

Patterns of Structural Changes in the Fundus Measured by Optical Coherence Tomography Angiography as Potential Markers of Acute Mountain Sickness

Yuancheng Zhao[1,*], Huan Zou[1,*], Wei Fan[1], Yuqi Liu[1], Xiaofan Chen[1], Yanming Huang[1], and Rongdi Yuan[1]

[1] Department of Ophthalmology, Second Affiliated Hospital of Army Medical University, Chongqing, China

Correspondence: Rongdi Yuan, Department of Ophthalmology, Second Affiliated Hospital of Army Medical University, 183#, Xinqiaozheng St., Shapingba District, Chongqing 400037, PR China. e-mail: yuanrongdi@126.com

Received: July 31, 2023
Accepted: November 3, 2023
Published: December 13, 2023

Keywords: optical coherence tomography angiography; acute mountain sickness; plateau hypoxia; retinal blood flow; choroid

Citation: Zhao Y, Zou H, Fan W, Liu Y, Chen X, Huang Y, Yuan R. Patterns of structural changes in the fundus measured by optical coherence tomography angiography as potential markers of acute mountain sickness. Transl Vis Sci Technol. 2023;12(12):15, https://doi.org/10.1167/tvst.12.12.15

Purpose: To use optical coherence tomography angiography (OCTA) to assess the pattern of changes in retinal and choroidal blood flow and structure in healthy volunteers who quickly went from sea level to a plateau and to determine the parameters associated with acute mountain sickness (AMS).

Methods: Forty-five individuals (89 eyes) were examined by OCTA and filled out the AMS questionnaire. One baseline examination was performed on the plain, followed by examinations at days 1, 3, and 5 after entering the plateau. Parameters were self-controlled to explore patterns of change, analyzed for correlation with AMS score, and modeled as a nomogram of AMS risk.

Results: On the plateau compared to the plain, vascular morphology showed dilated superficial macular retinal vessels and constricted deeper layers with increased vessel length density and fractal dimension; vessel density increased in all retinal strata and decreased in the choroidal macrovascular layer; and thickness increased except for a decrease in mean retinal thickness in the central macular sulcus. The rate of increase in retinal nerve fiber layer (RNFL) thickness in the inner and outer macular rings correlated with AMS score ($r = -0.211$). The nomogram showed moderate accuracy (AUC = 0.672) and consistency (C-index = 0.659) in assessing AMS risk.

Conclusions: In high-altitude hypoxia, retinal vessels dilate and distort, resulting in increased blood flow density and thickness. Increased RNFL thickness in the paracentral macula may be a marker of low AMS risk.

Translational Relevance: The changes in the retinal structure of the fundus can be used to assess the risk of developing AMS.

Introduction

Acute mountain sickness (AMS) usually occurs when people accustomed to lower altitudes are exposed to higher altitudes. The symptoms are mild and include headache, fatigue, nausea, and sleep disturbance, which can be relieved by oxygen and rest, but about 1% of cases can progress to acute illnesses such as pulmonary edema and cerebral edema,[1] requiring immediate descent to lower altitudes for treatment.[2] The number of people traveling to high altitudes for work has increased, and the incidence of AMS continues to rise,[3] so there is an urgent need for efficient and convenient methods to identify AMS and track the changes in its symptoms.

Human systems produce a series of physiological responses to adapt to high-altitude environments, such as increasing hemoglobin concentration, heart rate, and cardiac output to ensure oxygen supply to vital organs,[2] but no precise relationships with the changing course of AMS symptoms have been found, nor are they easy to monitor directly. The eye and the central nervous system have embryological and anatomical similarities, as they are the only areas with inner vasculature in the body that can be viewed directly, so

they can serve as a window to probe intracranial and systemic microcirculatory changes.[4] This vasculature can self-regulate to adapt to changes in oxygen partial pressure.[5] Previous studies have mainly tested hypoxia or hyperoxia by simulating it.[6,7] Few real-world studies of hypoxic environments in the plateau have been conducted. They have been limited to the study of one sublayer of the macula or optic disk, so the patterns of change in different regions and sublayers of the structure in hypoxic environments are inconclusive,[8,9] and investigating the correlation between changes in fundus tissues and the development of AMS has yielded little results.[10,11]

Therefore, we recruited healthy people who have lived at low altitude for a long time to fly to highland areas, where we innovatively used optical coherence tomography angiography (OCTA), a noninvasive, rapid, high-resolution method,[12] to explore the patterns of change in blood flow and thickness in various layers of the retina and choroid of the macula and optic papilla under the hypoxic environment of a highland. The results yielded ocular markers that might be associated with AMS changes. The results of the study can further our understanding of the human body's adaptation to high-altitude hypoxia through fundus changes and thus provide some guidance to high-altitude travelers.

Methods

Study Setting

This is a prospective observational study, approved by the Ethics Committee of the Second Affiliated Hospital of the Army Medical University (2022-Research No. 127-01) and filed in the Chinese Clinical Trials Registry (ChiCTR2200059834). It adhered to the tenets of the Declaration of Helsinki. All subjects signed a written consent form. The study ran from April to July 2022. One baseline examination was completed on the plain (Chongqing, 500 meters above sea level) 1 month before participants entered the plateau, followed by three plateau examinations on days 1, 3, and 5 after the participants were flown to the plateau (Tibet, 3874 meters above sea level). These examinations included OCTA, visual acuity, blood pressure, heart rate, oxygen saturation, and the Lake Louise Scoring (LLS) self-report questionnaire[13] (Supplementary Table S1). This study was conducted to explore the patterns and possible causes of changes in fundus retinal and choroidal blood flow and structure in healthy people after acute plateau entry, to analyze the correlation between ocular parameters and changes occurring in AMS, and to search for predictive markers of AMS by comparing the OCTA examination results of the participants' four measurements (Supplementary Fig. S1).

Subjects

Forty-five subjects (19 males, 26 females) underwent specialty examinations, including one subject whose examination revealed a choroidal hemangioma in the left eye, which was not included, leaving 89 eyes for analysis. Exclusion criteria included the following: (1) history of ocular disease or surgery; (2) uncontrolled hypertension, coronary heart disease, pregnancy, mental illness, or other conditions that would prevent adaptation to plateau activities; and (3) history of long-term residence on the plateau in the previous 6 months.

Measurements

Systemic Parameters

Subjects who completed the 2018 LLS questionnaire independently prior to each examination, who calculated a score of $\geq$3 total, and who had headache and at least one other symptom (dizziness, gastrointestinal distress, fatigue/weakness, and insomnia) were diagnosed with AMS[13] (Supplementary Table S1). Subjects rested in a seated position for 5 minutes. We used an automated blood pressure monitor (HEM-7200; Omron, Kyoto, Japan) to measure the left upper arm brachial blood pressure and heart rate. We measured right index finger oxygen saturation using a peripheral pulse oximeter (Onyx 9500 SportStat; Nonin Medical, Plymouth, MN).

Ocular Parameters

Best-corrected visual acuity was measured using a standard logarithmic visual acuity scale and was converted to the logarithm of the minimum angle of resolution visual acuity (logMAR VA). Both eyes were scanned using OCTA (DRI OCT Triton; Topcon, Tokyo, Japan), including macular 6 mm $\times$ 6 mm three-dimensional optical coherence tomography (3D-OCT) analysis of the retina, including the whole retina, retinal nerve fiber layer (RNFL), ganglion cell layer (GCL), and choroidal thickness. This included the central 1-mm-diameter circular area of the central macular concavity, 1- to 3-mm enclosed inner ring, 3- to 6-mm enclosed outer ring, measurement of the

centroid (where we measured the mean thickness of the central recess and the inner and outer rings), and the volume of the central macular depression[14] (Supplementary Figs. S2a, S2f). The choroidal vascular index (CVI) was analyzed by B-scan images of the macular central concavity obtained by manual analysis with ImageJ 1.53 (National Institutes of Health, Bethesda, MD) (Supplementary Fig. S2b).[15,16] Macular 3-mm × 3-mm blood flow imaging was used to analyze the retinal superficial capillary plexus (SCP), deep capillary plexus (DCP), and the whole retina; the sublayer of the retinal pigment epithelium (sub-RPE); and the choroidal capillary and macrovascular layers.

We quantified the mean vessel density (VD) in the central 1-mm circular central concave, the paracentral concave ring of 1 to 2.5 mm, and the foveal avascular zone (FAZ) area, as well as the perimeter and roundness of the SCP (Supplementary Figs. S2c, S2f). We performed 3.5-mm × 3.5-mm 3D-OCT of the optic papilla to analyze the mean thickness of retinal layers and choroid, optic disk, optic cup area, horizontal/vertical cup-to-disc ratio, and optic disk depression volume (Supplementary Figs. S2d, S2f). We analyzed blood flow density in a 2- to 4-mm ring around the 4.5-mm × 4.5-mm optic disk, including the radial peripapillary capillary (RPC), superficial, deep, and entire retinal layers, choroidal capillaries and macrovascular layer (Supplementary Table S2, Supplementary Fig. S2e). The 3-mm × 3-mm SCP and DCP blood flow maps of the macula were exported by the built-in system IMAGNET6 of the OCTA device, uniformly intercepted as square images with a side length of 250 pixels using MATLAB (MathWorks, Natick, MA), and cut and batch imported into an OCTA vascular analyzer.[17]

Noise reduction, binarization, and skeletonization were performed to derive four vascular morphological parameters: vessel length density (VLD), fractal dimension (FD), mean tortuosity (mTort), and mean vessel diameter (meanD) (Supplementary Fig. S3). We analyzed changes in the ratio of the full thickness and blood flow density of the inner retinal ring in the macula and the thickness and RPC density of the optic papilla RNFL to analyze the relationship between thickness changes and blood flow.[18] Finally, using the plains results as a baseline, the rate of change of each index was calculated for the three measurements on the plateau.

Reproducibility

To ensure consistency and accuracy of the assay, the same equipment was used on both the plain and the plateau. It was calibrated and tuned by engineers and only used after the parameters met the standards.[8] OCTA automatically searched and corrected the site through the eye anatomical feature tracking function for each image acquisition to produce a consistent image set.[19] Then, based on the subject's plain baseline parameters, the follow-on function was used with manual judgment to ensure that the same site was detected before and after. The above-mentioned use of MATLAB clipping also enhanced the comparability of the measurement results.[11] Analysis of the stratification results was corrected according to anatomical feature segmentation,[20] and only the system-set stratification boundaries were adjusted. The OCTA ratio analysis algorithm reduces motion artifact interference and improves the signal-to-noise ratio of the images,[21] yielding an image quality score of >55 for each examination. Finally, to exclude daily changes and environmental effects, all examinations were scheduled to be completed at the same time, in the same examination environment,[22] and by the same examiner. Each subject entered the examination room for 5 minutes of seated rest before the examination.

Statistical Analysis

SPSS Statistics 26 (IBM, Chicago, IL) was used for statistical analysis. All measurement data were tested using the Shapiro–Wilk test for normality and are expressed as median (quartile); count data are expressed as number (percentage). The repeated measures from the plain and the plateau on day 1, day 3, and day 5 (self-controls) were analyzed using the Friedman test with Bonferroni correction for two-way comparisons. The incidence of AMS was compared using the cross-tabulation χ^2 test. Only the right eye was considered when analyzing correlations, and the three measurements on the plateau of the same parameters were pooled for analysis. Correlations among the AMS score, rate of change in heart rate, and rate of change in oxygen saturation with the rate of change in OCTA parameters were analyzed using the Pearson correlation test.[8] The relationship between ocular parameters and the occurrence of AMS was analyzed using binary logistic regression, and receiver operating characteristic (ROC) curves were used to determine accuracy. The *rms* and *rmda* packages of RStudio 4.1.3 (R Foundation for Statistical Computing, Vienna, Austria) were used for the nomogram, calibration curves, and decision analysis curve. All tests were two tailed, with $P < 0.05$ indicating a significant difference. Graphs were plotted using Prism 8.1 (GraphPad, Boston, MA).

Results

A total of 45 (19 male, 26 female) subjects, 34 (28–39) years of age, completed the OCTA; 38 of them had all demographic parameters of interest. Heart rate, AMS score, and AMS incidence (73.68% on day 1, 47.37% on day 3, and 18.42% on day 5 of the plateau) significantly increased upon entering the plateau, with an overall mean AMS incidence of 46.5%. Oxygen saturation decreased ($P < 0.01$) on the plateau, but blood pressure and logMAR VA did not change significantly (Table 1).

Vascular Morphology

The mean vessel diameter of the macular retinal SCP increased and then decreased after entering the plateau ($P = 0.022$), and that of the DCP decreased significantly ($P = 0.002$). VLD and FD increased mildly in both the SCP and DCP but were only significant for the SCP. Mean tortuosity increased mildly in the SCP but was not significantly different from the plain value in the SCP or DCP. The FAZ area, circumference, and roundness of the macular SCP gradually decreased (Supplementary Table S3b).

Blood Flow Density

On the plateau, retinal SCP, DCP, and whole-layer blood flow density increased in the central macular recess and outer ring. Retinal RPC, SCP, DCP, and whole-layer density were also significantly higher in the region around the optic disk ($P < 0.001$). The choroidal RPE layer, capillaries, macrovascular layer, and CVI in the central macular sulcus showed a significant decrease in blood flow density on the plateau ($P < 0.01$), whereas the mean density of the outer ring did not change significantly. The change in choroidal capillary density in the region around the optic disk was not significant, but the macrovascular density decreased overall ($P < 0.01$).

Thickness of Structures

The volume of the central macular depression increased, but the volume of the optic papillary depression decreased; the area of the optic disk and optic cup increased; and both the horizontal and vertical cup-to-disc ratios decreased ($P < 0.001$). Retinal thickness decreased at the central point and fovea of the macula, but the mean thickness of the inner and outer rings increased, and the mean thickness of the retina, RNFL, GCL, and choroid in each of the remaining subdivisions produced subtle but significant increases ($P < 0.05$) (Table 2) (see Supplementary Tables S3a and S3b for changes in the upper and lower nasotemporal subdivisions) (Figs. 1A, 1B). There was no difference in the ratio of retinal thickening to blood flow density in the macula ($P = 0.103$), but there was a significant increase in RNFL/RPC in the region around the optic disk ($P = 0.007$) (Supplementary Table S4).

In the correlation analysis, only optic disk RPC blood flow density ($r = -0.205$, $P = 0.029$), inner macular ring thickness ($r = -0.211$, $P = 0.024$), outer ring RNFL thickness ($r = -0.211$, $P = 0.024$), and the rate of change in GCL inner ring thickness ($r = 0.211$, $P = 0.018$) correlated with AMS score. In the regression analysis with the occurrence of AMS as the dependent variable, the rate of change in the retinal RNFL

Table 1. Demographic Parameters ($n = 38$)

	Mean (95% CI)				
Parameters	Baseline	Day 1	Day 3	Day 5	*P*
HR (beats/min)	77.50 (72.00–83.25)	93.00 (84.75–105.00)[a]	91.50 (86.50–104.50)[a]	87.50 (79.50–94.25)[a,b]	0.000
MAP (mmHg)	85.67 (80.00–90.33)	85.50 (78.17–95.67)	87.33 (78.58–93.00)	88.00 (80.83–97.42)	0.703
SBP	110.50 (102.75–120.25)	113.50 (102.00–125.25)	113.50 (102.50–122.25)	115.50 (103.75–124.50)	0.239
DBP	73.00 (68.00–77.50)	73.00 (65.75–81.25)	73.00 (66.75–79.25)	75.00 (69.75–83.25)	0.295
SpO_2 (%)	97.00 (96.00–98.00)	88.00 (84.75–90.00)[a]	88.00 (83.75–91.00)[a]	89.50 (88.75–91.00)[a]	0.000
AMS scores	0	3.00 (2.00–4.25)[a]	2.50 (0.75–4.00)[a]	1.00 (0.00–2.00)[a,b]	0.000
AMS (%)	0	28 (73.68)	18 (47.37)	7 (18.42)	0.000
LogMar VA[c]	0.00 (0.00–0.14)	0.03 (−0.05–0.10)	0.03 (−0.05–0.10)	0.03 (−0.05–0.10)	0.506

MAP = 1/3 SBP + 2/3 DBP. CI, confidence interval; DBP, diastolic blood pressure; HR, heart rate; logMAR VA, logarithm of the minimum angle of resolution visual acuity; MAP, mean arterial pressure; SBP, systolic blood pressure; SpO_2, oxygen saturation.

[a]Comparison with the plain.

[b]Comparison with the first day of the plateau.

[c]If a parameter marked with a superscript of a, b, the difference between the two groups is statistically significant; if not, it means none. Sample size was 89 eyes.

Table 2. Analysis of Blood Flow and Structure Changes in Macula and Optic Papilla ($n = 89$)

Parameters	Mean (95% CI) Baseline	Day 1	Day 3	Day 5	*P*
Macular blood flow image analyzed by OCTA vascular analyzer					
VLD (%)					
SCP	3.91 (3.75–4.10)	3.94 (3.80–4.11)	4.03 (3.86–4.18)	4.05 (3.83–4.18)	0.016
DCP	3.66 (3.46–3.91)	3.73 (3.52–3.91)	3.72 (3.61–3.96)	3.78 (3.60–3.94)	0.102
FD, none					
SCP	1.54 (1.52–1.55)	1.54 (1.52–1.55)	1.54 (1.53–1.55)	1.54 (1.53–1.55)[a]	0.016
DCP	1.55 (1.54–1.56)	1.55 (1.54–1.56)	1.55 (1.54–1.56)	1.55 (1.55–1.56)	0.066
MeanD (μm)					
SCP	43.50 (38.00–55.25)	45.00 (39.00–57.00)	44.00 (38.00–55.25)	41.00 (37.00–47.00)[a]	0.022
DCP	40.00 (36.00–46.00)	40.00 (36.00–45.00)	38.00 (34.00–42.00)	37.00 (33.00–41.00)[a,b]	0.002
mTort, none					
SCP	0.14 (0.13–0.16)	0.15 (0.13–0.17)	0.14 (0.13–0.16)	0.14 (0.13–0.16)	0.254
DCP	0.14 (0.13–0.16)	0.13 (0.13–0.15)	0.14 (0.13–0.16)	0.14 (0.13–0.16)	0.412
Vessel density (%)					
Macular center					
SCP	18.75 (16.23–21.99)	19.90 (17.75–22.82)[b]	20.19 (18.13–23.21)[b]	20.33 (18.18–22.48)[b]	0.000
DCP	14.35 (10.81–17.46)	15.31 (12.71–18.67)	15.81 (13.56–19.97)[b]	17.28 (14.80–21.31)[a,b]	0.000
Total retina	17.95 (15.25–20.54)	18.53 (16.78–21.11)[b]	19.00 (17.15–21.78)[b]	18.95 (17.10–21.39)[b]	0.000
Sub-RPE	54.59 (52.74–56.16)	53.00 (51.38–54.67)[b]	53.30 (51.54–54.96)[b]	52.62 (50.94–54.43)[b]	0.000
Choriocapillaris	54.32 (52.49–55.98)	53.69 (51.60–55.47)	53.24 (51.86–55.36)[b]	53.30 (51.85–55.09)[b]	0.004
Choroidal vessels	55.71 (51.89–57.80)	55.17 (50.92–58.47)	54.53 (51.06–57.61)	53.57 (50.12–56.83)[a,b]	0.004
CVI	65.32 (64.44–66.69)	64.00 (62.95–65.20)[b]	64.19 (63.25–65.26)[b]	64.16 (63.38–65.41)[b]	0.000
Paracentral fovea					
SCP	48.68 (47.18–50.12)	50.20 (49.13–51.38)[b]	50.41 (49.25–51.41)[b]	50.52 (49.66–51.38)[b]	0.000
DCP	48.72 (47.21–50.14)	50.19 (48.83–51.21)[b]	50.13 (48.95–51.12)[b]	49.88 (48.98–50.94)[b]	0.000
Total retina	51.37 (50.37–52.41)	52.65 (51.63–53.63)[b]	52.75 (51.62–53.41)[b]	52.39 (51.63–53.20)[b]	0.000
Sub-RPE	53.42 (52.58–54.13)	53.41 (52.75–54.18)	53.32 (52.80–54.12)	53.43 (52.82–53.95)	0.412
Choriocapillaris	53.54 (52.95–54.10)	53.21 (52.77–53.96)	53.45 (52.68–54.10)	53.34 (52.72–53.96)	0.368
Choroidal vessels	52.06 (51.15–53.13)	51.96 (50.96–53.21)	51.94 (51.08–52.91)	51.91 (50.81–53.02)	0.153
Peripapillary optic					
RPC	49.13 (47.72–50.41)	50.91 (49.55–52.09)[b]	50.76 (49.19–51.68)[b]	51.06 (49.77–51.83)[b]	0.000
SCP	49.41 (47.70–50.58)	51.22 (49.82–52.22)[b]	50.86 (49.15–51.81)[b]	51.10 (50.16–52.02)[b]	0.000
DCP	41.96 (39.26–44.04)	44.84 (43.09–46.21)[b]	44.40 (43.04–46.17)[b]	44.71 (43.21–46.23)[b]	0.000
Total optic	48.90 (47.37–50.09)	50.47 (49.42–51.52)[b]	50.43 (48.54–51.37)[b]	50.59 (49.62–51.42)[b]	0.000
Choriocapillaris	59.04 (57.95–60.48)	59.23 (57.96–59.97)	58.91 (57.96–59.97)	59.08 (58.07–60.08)	0.141
Choroidal vessels	62.20 (60.60–63.68)	61.96 (60.25–63.53)	61.62 (60.35–62.93)[b]	61.64 (60.06–63.07)[b]	0.002
Thickness (μm)					
ART					
Central	180.00 (171.50–190.00)	180.00 (170.00–187.00)[b]	179.00 (169.00–190.00)[b]	178.00 (168.00–188.00)[b,c]	0.000
Macular region	229.00 (219.50–239.50)	227.00 (216.00–237.00)[b]	228.00 (217.00–238.00)[b]	226.00 (215.00–237.50)[a–c]	0.000
Inner concave	307.00 (298.38–318.13)	306.75 (299.25–319.50)	307.75 (299.63–318.63)	305.75 (299.00–317.50)[a–c]	0.000
Outer concave	271.75 (263.63–281.75)	273.00 (265.88–282.00)[b]	273.00 (265.75–282.50)[b]	272.00 (263.88–281.25)[c]	0.000
Optic	296.75 (284.25–307.13)	299.50 (290.13–313.38)[b]	301.75 (290.25–312.88)[b]	302.00 (290.13–315.63)[a,b]	0.000
ACT					
Macular region	234.00 (195.00–304.50)	226.00 (186.50–306.00)	237.00 (197.50–316.00)[a,b]	234.00 (198.00–317.50)[a,b]	0.000
Inner concave	228.50 (196.63–297.13)	224.25 (192.50–298.13)	230.00 (196.63–308.25)[a,b]	232.25 (200.75–302.13)[a,b]	0.000
Outer concave	219.00 (189.50–260.50)	217.25 (184.88–262.00)	223.75 (187.00–266.75)[a,b]	218.00 (193.25–266.38)[a,b]	0.000
Optic	144.50 (117.50–172.25)	144.50 (113.86–174.75)	147.75 (118.63–176.00)[b]	148.75 (119.75–177.75)[a,b]	0.000
ARNFL					
Inner concave	25.50 (24.50–27.25)	25.75 (25.00–27.75)[b]	26.25 (25.25–27.75)[a,b]	26.25 (24.75–27.50)[b]	0.000
Outer concave	40.50 (37.88–42.50)	41.50 (39.00–43.50)[b]	42.00 (39.63–44.00)[a,b]	42.25 (39.50–44.25)[a,b]	0.000
Optic	112.00 (104.13–116.63)	115.50 (107.88–120.25)[b]	116.75 (109.25–122.13)[b]	116.50 (108.25–123.25)[a,b]	0.000
AGCL+					
Macular region	41.00 (37.00–46.00)	43.00 (38.00–47.00)[b]	43.00 (38.00–47.00)[b]	42.00 (37.50–47.00)[b]	0.000
Inner concave	92.00 (88.13–96.13)	93.50 (89.63–97.25)[b]	93.75 (90.25–96.88)[b]	93.75 (89.75–97.25)[b]	0.000
Outer concave	67.75 (63.00–69.88)	68.25 (64.88–70.50)[b]	68.00 (64.88–70.75)[b]	68.25 (64.75–71.25)[b]	0.000
Optic	42.25 (39.63–44.50)	42.75 (39.75–45.50)	42.50 (40.25–45.00)[b]	42.50 (39.75–46.13)[b]	0.000

ART, average retinal thickness; ACT, average choroidal thickness; ARNFL, average retinal nerve fiber layer; AGCL, average ganglion cell layer.

[a]Comparison with the first day of the plateau.

[b]Comparison with the plain.

[c]Comparison with the third day of the plateau. If a parameter marked with a superscript of a, b, c, the difference between the two groups is statistically significant; if not, it means none.

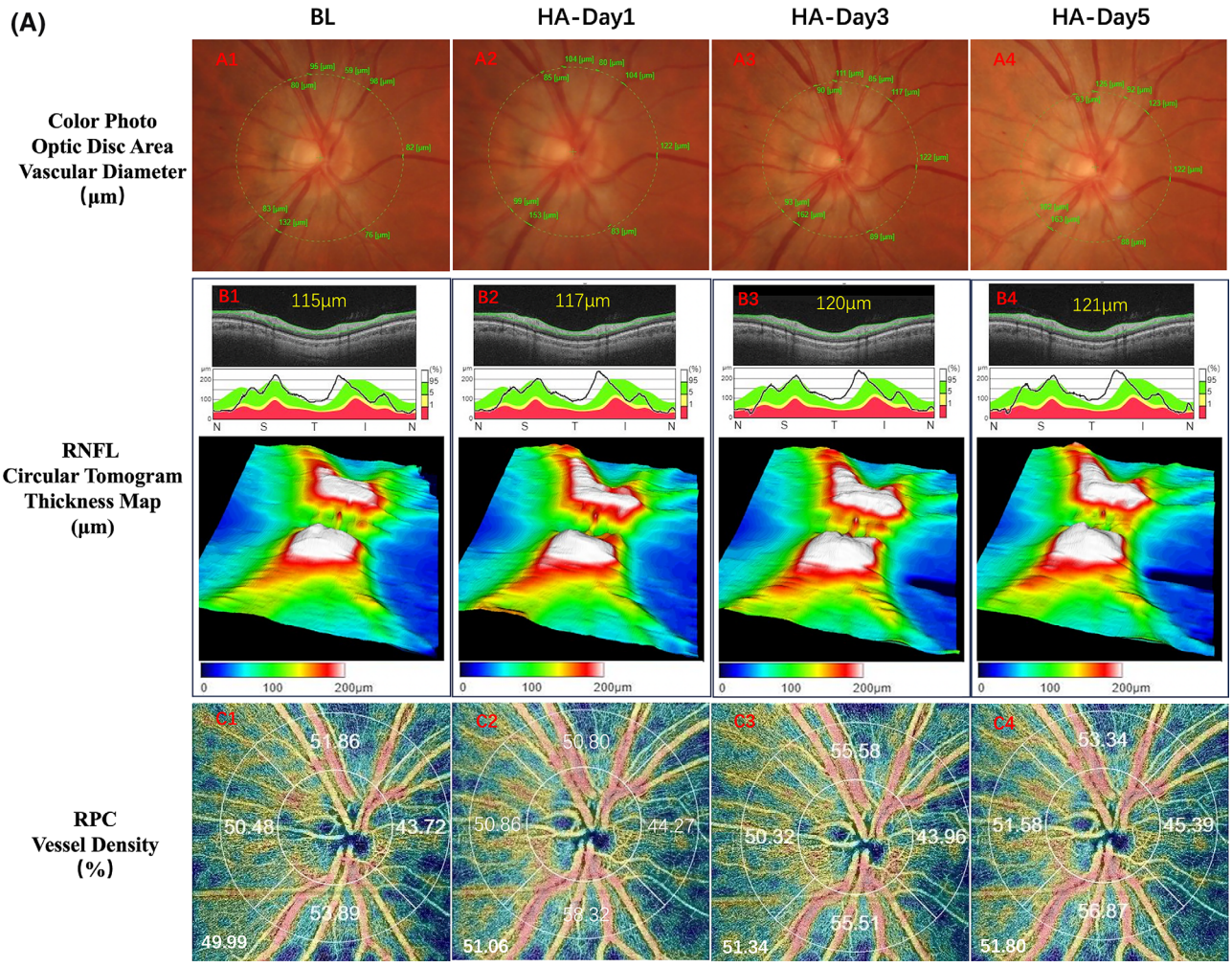

Figure 1. (**A**) Map of tissue thickness and blood flow density changes in the optic disk region. From *left to right*, the images are at the baseline level of the plain and on the first day, third day, and fifth day after entering the plateau, respectively. The *first row*, A1 to A4, shows the fundus color photographs of the optic disk region; the diameters of the retinal branch arterioles were measured by the built-in software of the instrument, and it can be seen that the vessel diameters of the arterioles increased significantly after entering the plateau. The *second row*, B1 to B4, shows the thickness measurements of the nerve fiber layer of the optic disk, and it can be seen in the numerical values and the three-dimensional thickness thermograms that the thickness of the RNFL increased gradually after participants entered the plateau. The *third row*, C1 to C4, shows the thickness of the peripheral capillaries of the optic disk. Row C4 shows the blood flow density maps of the peripapillary network around the optic disk, which also increased gradually after entering the plateau. (**B**) Map of tissue thickness and blood flow density changes in the macular region. The *first row*, A1 to A4, shows the three-dimensional thickness maps of the macular central concavity region. The volume of the central concavity is labeled in the *lower left corner*; it gradually increased upon entry into the plateau. The *second row*, B1 to B4, shows the RNFL thickness maps of the macular region. The *green* R1 in the lower left corner indicates the average thickness of the inner ring of the region around the optic disk concavity, and the *red* R2 in the lower left corner is the average thickness of the outer ring. It can be seen that the RNFL thickness increased gradually after exposure to the plateau. The *third row*, C1 to C4, shows the SCP with macular diameter of 2.5 mm; the images were processed by OCTAVA binarization to calculate the average vessel diameter within the image, which gradually increased after entering the plateau, indicating that the blood vessels were dilated to a certain extent. The *fourth row*, D1 to D4, shows the skeletonization of the third row of the images, and the vessel length density (VLD) was calculated, which can be seen to gradually increase in the plateau environment. The *fifth row*, E1 to E4, shows the blood flow density maps of the macular region, which are analyzed automatically by the instrument; the average blood flow density of the paracentral notch ring is shown in the *lower left corner*, which also increases gradually with entry. BL, baseline; HA, high altitude; ILM, inner limiting membrane.

inner ring thickness (odds ratio [OR] = 0.854, P = 0.010) and the rate of change in outer ring thickness (OR = 0.835, P = 0.023) were statistically significant. The ROC analysis of the inner ring (area under the ROC curve [AUC] = 0.645, P = 0.008) and outer ring (AUC = 0.672, P = 0.002) had moderate accuracy. For every 1-unit increase in the rate of change in the thickness of the RNFL, there was an overall decrease in the

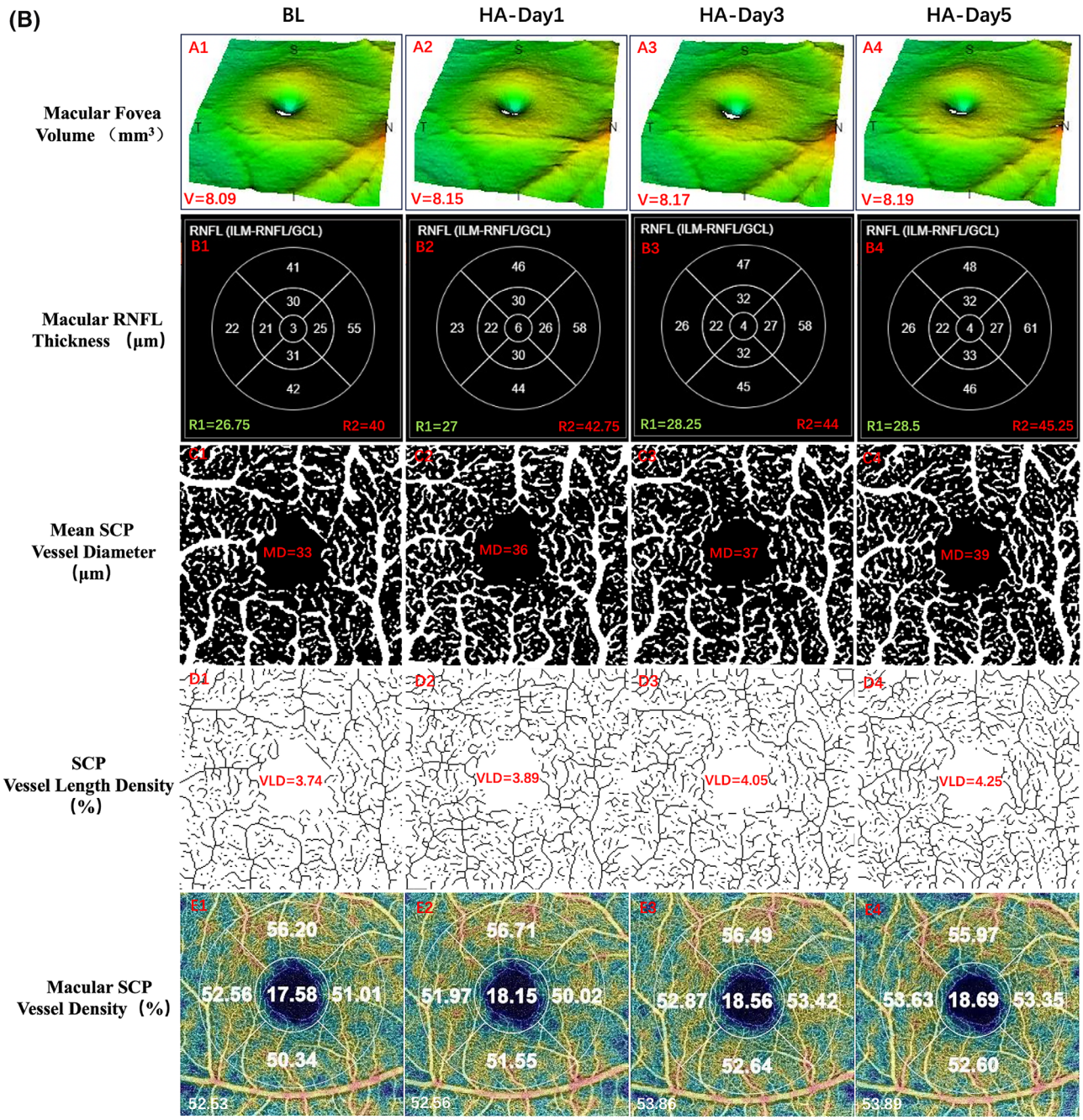

Figure 1. Continued.

AMS score of 0.374 (inner ring) or 0.288 (outer ring) (Fig. 2). The RPC ($P = 0.085$) and the inner retinal ring GCL ($P = 0.273$) did not have statistically significant relationships with AMS occurrence (Table 3). The choroidal thickness growth rate in the central macular recess ($r = -0.272$, $P = 0.003$) and region around the optic disk ($r = -0.366$, $P < 0.001$) were negatively correlated with the rate of heart rate change. The rate of decrease in final oxygen saturation was positively correlated with the rates of increase in the thickness of the inner macular ring ($r = 0.214$, $P = 0.022$), the outer ring ($r = 0.230$, $P = 0.014$), the region around the optic disk RNFL ($r = -0.222$, $P = 0.017$), and the outer macular ring GCL ($r = -0.237$, $P = 0.011$). The rate of decrease in final oxygen saturation was negatively correlated with the rates of increase in the superficial macular central recess VD ($r = -0.238$, $P = 0.011$) (Supplementary Table S5). Figure 3 demonstrates a nomogram model of the rate of change of the RNFL in the inner and outer macular rings versus

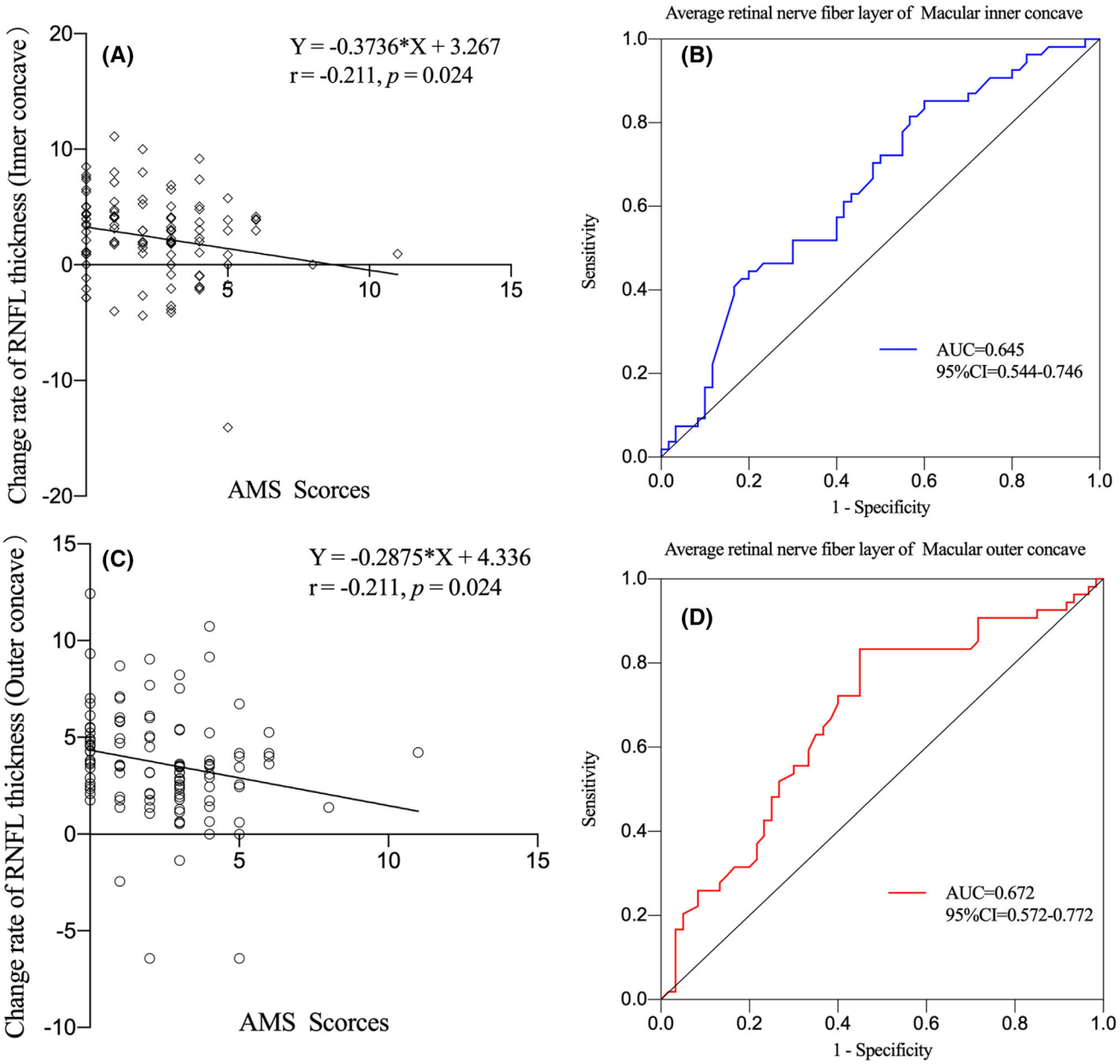

Figure 2. Correlation analysis of the rate of increase in macular inner and outer ring thickness with the occurrence of change in AMS. (**A**, **C**) Correlations between the rate of change of macular inner and outer ring RNFL thickness and AMS score; both have significant but weak correlations. It can be seen that, for every 1 unit increase in the thickness change rate of RNFL, the overall AMS score decreased by 0.3736 (inner ring) or 0.2875 (outer ring). (**B**, **D**) Graphs show the ROC curve analysis of the two parameters with the occurrence of AMS, which indicates that the rate of thickening of macular RNFL has some ability to identify the occurrence of AMS.

the risk of AMS. It had a calibration curve C-index of 0.659. The decision analysis curve (Supplementary Fig. S4) suggested that the model is applicable for AMS risk thresholds in the range of 10% to 28%.

Discussion

Our study found small but significant patterns of changes in retinal and choroidal vessel morphology (diameter, length, tortuosity), blood flow density, and histology (thickness, area, and volume) in the macula and the region around the optic disk in a healthy population living at low altitude who enter a plateau hypoxic environment. The rate of change in RNFL thickness in the inner and outer macular rings was negatively correlated with AMS score, which has some accuracy in determining AMS, and ocular markers correlated with heart rate and oxygen saturation were found. These findings will

Table 3. Correlation Analysis Between Change Rate of OCTA Parameters and AMS Scores and Regression Analysis for Whether AMS Occurs ($n = 114$)

Parameters	*r* (95% CI)	*P*	OR (95% CI)	*P*
SCP VLD	−0.063 (−0.244∼0.123)	0.507	1.009 (0.996∼1.053)	0.699
SCP FD	−0.003 (−0.186∼0.181)	0.978	1.031 (0.867∼1.225)	0.731
SCP meanD	−0.030 (−0.213∼0.155)	0.751	0.998 (0.988∼1.007)	0.656
DCP	−0.025 (−0.208∼0.160)	0.794	1.004 (0.989∼1.020)	0.567
Vessel density				
Macular central				
CVI	0.005 (−0.179∼0.189)	0.957	0.991 (0.881∼1.116)	0.887
SCP	0.093 (−0.093∼0.272)	0.326	1.007 (0.974∼1.042)	0.681
DCP	−0.020 (−0.204∼0.164)	0.829	0.998 (0.990∼1.007	0.705
Total retina	0.112 (−0.073∼0.290)	0.235	1.007 (0.977∼1.037)	0.663
Sub-RPE	0.070 (−0.116∼0.250)	0.461	0.993 (0.924∼1.066)	0.993
Choriocapillaris	0.059 (−0.126∼0.241)	0.532	0.968 (0.895∼1.048)	0.423
Choroidal vessels	0.018 (−0.116∼0.202)	0.847	0.992 (0.937∼1.050)	0.786
Macular paracentral				
SCP	0.032 (−0.153∼0.214)	0.738	1.011 (0.935∼1.093)	0.789
DCP	0.018 (−0.166∼0.202)	0.846	0.980 (0.906∼1.059)	0.607
Total retina	0.074 (−0.111∼0.255)	0.433	1.077 (0.924∼1.255)	0.344
Optic				
RPC	−0.205 (−0.375∼−0.022)	0.029	0.905 (0.807∼1.014)	0.085
SCP	−0.148 (−0.323∼0.037)	0.117	0.945 (0.862∼1.036)	0.230
DCP	−0.122 (−0.299∼0.064)	0.198	0.981 (0.956∼1.008)	0.162
Total retina	−0.128 (−0.305∼0.057)	0.174	0.949 (0.860∼1.046)	0.292
Choroidal vessel	−0.048 (−0.229∼0.138)	0.616	0.934 (0.803∼1.085)	0.371
Thickness				
ART				
Central	0.083 (−0.102∼0.263)	0.380	1.035 (0.889∼1.205)	0.658
Macular region	−0.057 (−0.238∼0.129)	0.548	0.921 (0.749∼1.132)	0.432
Inner concave	0.009 (−0.175∼0.193)	0.925	0.999 (0.687∼1.452)	0.994
Outer concave	−0.131 (−0.307∼0.055)	0.165	0.820 (0.595∼1.130)	0.225
Optic	−0.119 (−0.297∼0.066)	0.206	0.906 (0.717∼1.145)	0.409
ACT				
Macular region	−0.172 (−0.345∼0.012)	0.067	0.975 (0.936∼1.016)	0.223
Inner concave	−0.150 (−0.325∼0.034)	0.110	0.972 (0.924∼1.023)	0.278
Outer concave	−0.104 (−0.283∼0.081)	0.270	0.979 (0.925∼1.036)	0.467
Optic	−0.153 (−0.328∼0.032)	0.104	0.955 (0.906∼1.006)	0.955
ARNFL				
Inner concave	−0.211 (−0.380∼−0.028)	0.024	0.854 (0.757∼0.963)	0.010
Outer concave	−0.211 (−0.380∼−0.028)	0.024	0.835 (0.715∼0.976)	0.023
Optic	−0.050 (−0.232∼0.135)	0.597	0.973 (0.903∼1.047)	0.463
AGCL+				
Inner concave	0.211 (0.039∼0.389)	0.018	1.107 (0.923∼1.328)	0.273
Outer concave	−0.005 (−0.189∼0.179)	0.961	1.114 (0.828∼1.500)	0.475
Optic	0.010 (−0.174∼0.194)	0.913	1.017 (0.958∼1.079)	0.586

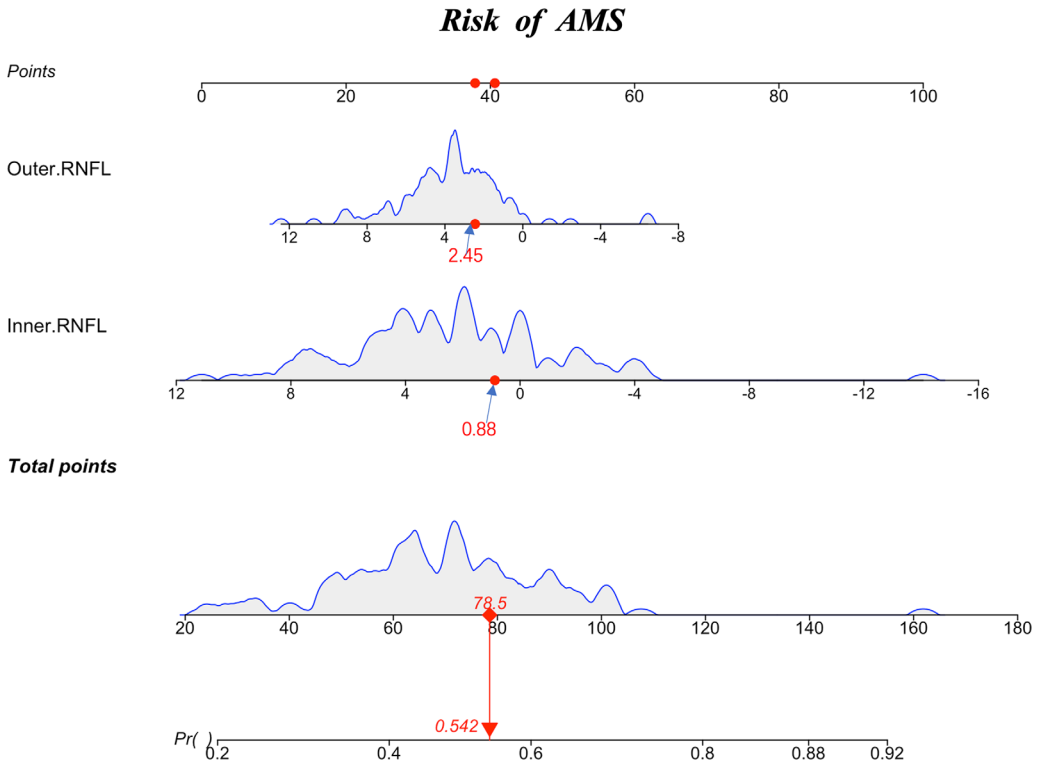

Figure 3. Risk nomogram of whether AMS has occurred. The rate of change from baseline in the thickness of the inner and outer rings of the RNFL in one randomized subject was 0.88 (score 40.5) and 2.45 (score 38), for a total score of 78.5, which corresponds to a risk of 54.2% of possibly having AMS. With the increase in the rate of change, the corresponding score decreased and the risk of AMS decreased, which can be seen as a guide to the occurrence of AMS and can serve the clinic better.

help explain the self-regulatory, adaptive changes that occur in the human body after an acute altitude increase.

The fundus has two systems, the retina and the choroid, the former being mainly regulated by local metabolism with low blood flow and high oxygen extraction[23] and the latter being innervated by autonomic nerves with a high perfusion rate and low oxygen consumption.[24] We found an increase in macular SCP vessel diameter during hypoxia, as has been reported previously,[25,26] probably due to altered vascular permeability and local production of vasoactive mediators.[23] Because retinal SCP and DCP vasculatures respond to changes in oxygen partial pressure differently and regulate by different mechanisms,[27] experiments in simulated hyperoxia and hypoxia have found that contraction of the DCP is more pronounced in hyperoxic environments, whereas the diastole of the SCP is more pronounced in hypoxic environments, possibly explaining the dilatation of our SCP and the contraction of our DCP.[6] The exact mechanism is not clear. It has been stated that an increase in tortuosity suggests pathological microvascular remodeling or ischemia.[17] Additionally, the FD is an objective parameter for assessing microvascular morphology; for example, when observing the progression of diabetic retinopathy (DR),[28] a decrease in FD indicates a worsening of the DR.[29] Therefore, in our results, the unchanged tortuosity of the SCP and the significant increase in FD in the presence of hypoxia on the plateau suggest that the healthy fundus vasculature can counteract the changes in hypoxia by self-regulation. Finally, the reduction in area and circumference of the FAZ in the superficial macula was mainly due to an increase in vessel diameter, whereas the decrease in roundness indicated some concomitant vascular distortion. Consistent with previous studies,[24,25,30] we found increased blood flow density in the retinal macula and parafoveal retinal layers. In particular, although the macular retinal DCP vessel diameter decreased, blood flow density increased because vessel density is defined as the percentage of blood flow pixels out of the total area.[12,31,32] This suggests that the total vascular area per unit area may be increased by increasing vessel complexity and length density.[33] In contrast to the retina, blood flow density in the choroid tended to decrease, mainly because of the anatomical and functional differences between the two.[34] The

choroidal arteries are surrounded by autonomic fiber plexuses and are largely unaffected by changes in external oxygen partial pressure.[35] One study found that choroidal blood flow density decreased with cold pressor testing and breath-hold hypoxia and increased with hyperoxia and hyperventilation, suggesting a negative correlation between the excitability of sympathetic activity and choroidal blood flow density.[19]

Changes in vascular morphology and blood flow density were reflected in structural changes. The thickness of all retinal layers in the inner and outer macular rings and region around the optic disk increased due to the increase in the blood flow density supplying them.[36] A positive correlation between retinal thickness and vascular changes has been reported.[37] Our comparison of the ratio of macular thickness to blood flow density found no change between measurements, suggesting that the increase in thickness could be explained by blood flow density. However, the increase in thickness of the region around the optic disk RNFL was significantly greater than that of the RPC, suggesting that, in addition to vascular changes, there was edema of the RNFL itself.[38] The decrease in retinal thickness in the central macular sulcus may be due to the absence of blood vessels in this region, with thinning in the middle and thickening in the periphery finally leading to an increase in the volume of the central macular sulcus. One study found that the increase in optic nerve sheath diameter reflects hypoxia-driven optic papilla edema formation, resulting in a decrease in the volume of the optic disk depression.[9] Therefore, our observation of an enlarged optic disk may be due to blurring of the edges of the optic disk due to edema, but it does not meet the criteria for a clinical diagnosis, and, as the edema subsides, the optic disk area and diameter will decrease[14] (Supplementary Fig. S5). Consistent with other studies, the choroidal thickness of both the macula and the region around the optic disk increased,[10] which may be due to metabolic edema in the hypoxic state[39] and may be similar to plateau cerebral edema[40]; however, blood flow density decreased. Because OCTA does not provide direct information on blood flow volume,[41] we calculated the cross-sectional CVI, which showed a decrease in choroidal vascular density, suggesting that choroidal vasoconstriction and edema of the canal wall and surrounding tissues result in increased thickness.[15]

The retinal vasculature can autoregulate in response to environmental stimuli.[5] However, compensatory regulation is limited, and exceeding the threshold will fail to compensate, a major cause of retinal disease.[37] Effective regulation ensures normal retinal function.[24] Our study found that the rate of increase in RNFL thickness in the inner and outer macular rings was negatively correlated with AMS score in healthy people in hypoxic environments and was accurate for determining the occurrence of AMS, suggesting that an appropriate conditioning response to hypoxia on the plateau predicts a better adaptation to the environment and weaker AMS symptoms. According to the nomogram (Fig. 3), the rates of change of the thickness of the inner and outer rings of the RNFL in one random subject were 0.88 (score 40.5) and 2.45 (score 38), respectively, totaling 78.5, which corresponds to a possible risk of AMS of 54.2%. As the rate of change increases, the corresponding score decreases and the risk of AMS decreases, so it has a certain role in guiding whether AMS occurs, and it can serve the clinic better.

Vascular reactivity to human eye stimulation has become a distinction between health and disease, and the severity of impaired vascular reactivity can be used to monitor disease progression or assess treatment.[42] For example, uncontrolled overperfusion in the early stages of DR suggests that a decrease in autoregulatory capacity plays an important role in pathogenesis.[27,43] Under plateau hypoxia, healthy people have increased cardiac output, increased heart rate, and decreased SpO_2, and blood pressure may also be slightly elevated temporarily,[44] all partially recovered during acclimatization.[45] Our results indicate that blood pressure remained stable, as only one subject experienced elevated blood pressure after exercise, which returned to normal upon return to the plain. However, individuals with cardiovascular and respiratory disease have a higher likelihood of developing AMS because of reduced reserve regulation in response to hypoxic environments.[46] Also, dysregulation of the sympathetic nervous system and metabolic vascular control is associated with severe cardiopulmonary disease and often precedes clinical symptoms.[47,48] Therefore, it is interesting that we found ocular parameters associated with changes in heart rate and oxygen saturation that indirectly reflect the activity of the systemic autonomic nervous system. Changes in the retina and choroid reflect the activity of different regulatory mechanisms. Because of its high resolution, noninvasive quantification,[49,50] and reproducibility,[14,51] OCTA has the ability to differentiate between the choroid and the retina,[19] allowing the detection of subtle changes in the vasculature. This enables it to reflect the local metabolic and neurological status of the whole body by fundus changes.[42]

Based on our results, we suggest that healthy people can predict their degree of AMS by testing the structural reactivity of the fundus through a hypoxia test before going to a higher altitude. After they enter a plateau, we can track their status in real time by

observing the fundus reaction, which can serve as a window into the changes in whole-body hypoxia. These measures can offer valuable guidance to travelers headed to high-altitude areas.

Limitations

Although we were well prepared, there were some shortcomings to this study. First, because OCTA measurements had never been performed in such an environment, systematic errors could not be completely ruled out, but we were very careful to calibrate the light source and other factors according to the manufacturer's comprehensive instructions.[8] Second, because of technical limitations, vessel diameter and torsion could not be analyzed in the choroid and optic papilla. Our vessel density was fixed with built-in stratification boundaries and could have been affected by individual differences, but our comparisons were repeated measurements of our own controls, and segmentation line correction was performed separately for each scan when analyzing each stratification index.[20] Third, the AMS risk nomogram does not have high consistency or applicability, and further research is needed to improve its clinical applicability. Finally, the age range of the research subjects was relatively narrow. Although the sample size was larger than earlier ones, the validity of the results must be verified by additional studies.

Conclusions

We identified the patterns of vascular and structural changes in the different layers and regions of the retina and choroid under hypoxic conditions in a real plateau hypoxic environment using OCTA, a safe, convenient, quantitative, reliable technology. The measurements indirectly reflected the role of sympathetic nerves and local metabolism in the regulation of ocular vasculature, providing a large amount of real-world data. In particular, increased RNFL thickness in the paracentral macula was identified as a potential marker for the development of AMS, as were ocular parameters associated with changes in heart rate and oxygen saturation. These features can serve as a window into the hypoxic damage to the brain and the whole body.

Acknowledgments

The authors thank Xiong Xiangwei, Bai Lian, Luo Lei, Qing Lu, and Wan Jun for their dedication to recruiting people and coordinating materials. We also thank the participants in this study and their relatives. None of these individuals was compensated for their contributions.

Disclosure: **Y. Zhao**, None; **H. Zou**, None; **W. Fan**, None; **Y. Liu**, None; **X. Chen**, None; **Y. Huang**, None; **R. Yuan**, None

* YZ and HZ contributed equally to this article.

References

1. Jin J. Acute mountain sickness. *JAMA*. 2017;318(18):1840.
2. Nuss R. Medical conditions and high-altitude travel. *N Engl J Med*. 2022;386(19):1866.
3. Keyes LE, Mather L, Duke C, et al. Older age, chronic medical conditions and polypharmacy in Himalayan trekkers in Nepal: an epidemiologic survey and case series. *J Travel Med*. 2016;23(6):taw052.
4. Wilson MH, Newman S, Imray CH. The cerebral effects of ascent to high altitudes. *Lancet Neurol*. 2009;8(2):175–191.
5. Cheng RW, Yusof F, Tsui E, et al. Relationship between retinal blood flow and arterial oxygen. *J Physiol*. 2016;594(3):625–640.
6. Hommer N, Kallab M, Sim YC, et al. Effect of hyperoxia and hypoxia on retinal vascular parameters assessed with optical coherence tomography angiography. *Acta Ophthalmol*. 2022;100(6):e1272–e1279.
7. Linsenmeier RA, Zhang HF. Retinal oxygen: from animals to humans. *Prog Retin Eye Res*. 2017;58:115–151.
8. Fischer MD, Willmann G, Schatz A, et al. Structural and functional changes of the human macula during acute exposure to high altitude. *PLoS One*. 2012;7(4):e36155.
9. Schatz A, Guggenberger V, Fischer MD, et al. Optic nerve oedema at high altitude occurs independent of acute mountain sickness [Published online ahead of print July 4, 2018]. *Br J Ophthalmol*, https://doi.org/10.1136/bjophthalmol-2018-312224.
10. Fischer MD, Schatz A, Seitz IP, et al. Reversible increase of central choroidal thickness during high-altitude exposure. *Invest Ophthalmol Vis Sci*. 2015;56(8):4499–4503.
11. Willmann G, Fischer MD, Schatz A, et al. Quantification of optic disc edema during exposure to

high altitude shows no correlation to acute mountain sickness. *PLoS One*. 2011;6(11):e27022.
12. Spaide RF, Fujimoto JG, Waheed NK, Sadda SR, Staurenghi G. Optical coherence tomography angiography. *Prog Retin Eye Res*. 2018;64:1–55.
13. Roach RC, Hackett PH, Oelz O, et al. The 2018 Lake Louise Acute Mountain Sickness score. *High Alt Med Biol*. 2018;19(1):4–6.
14. Ascaso FJ, Nerín MA, Villén L, Morandeira JR, Cristóbal JA. Acute mountain sickness and retinal evaluation by optical coherence tomography. *Eur J Ophthalmol*. 2012;22(4):580–589.
15. Agrawal R, Ding J, Sen P, et al. Exploring choroidal angioarchitecture in health and disease using choroidal vascularity index. *Prog Retin Eye Res*. 2020;77:100829.
16. Goud A, Singh SR, Sahoo NK, et al. New insights on choroidal vascularity: a comprehensive topographic approach. *Invest Ophthalmol Vis Sci*. 2019;60(10):3563–3569.
17. Untracht GR, Matos RS, Dikaios N, et al. OCTAVA: an open-source toolbox for quantitative analysis of optical coherence tomography angiography images. *PLoS One*. 2021;16(12):e0261052.
18. Sung JY, Lee MW, Lim HB, Ryu CK, Yu HY, Kim JY. The ganglion cell–inner plexiform layer thickness/vessel density of superficial vascular plexus ratio according to the progression of diabetic retinopathy. *Invest Ophthalmol Vis Sci*. 2022;63(6):4.
19. Jendzjowsky NG, Steinback CD, Herman RJ, Tsai WH, Costello FE, Wilson RJA. Functional-optical coherence tomography: a non-invasive approach to assess the sympathetic nervous system and intrinsic vascular regulation. *Front Physiol*. 2019;10:1146.
20. Oberwahrenbrock T, Weinhold M, Mikolajczak J, et al. Reliability of intra-retinal layer thickness estimates. *PLoS One*. 2015;10(9):e0137316.
21. Stanga PE, Tsamis E, Papayannis A, Stringa F, Cole T, Jalil A. Swept-Source Optical Coherence Tomography Angio (Topcon Corp, Japan): technology review. *Dev Ophthalmol*. 2016;56:13–17.
22. Clarke AK, Cozzi M, Imray CHE, Wright A, Pagliarini S. Analysis of retinal segmentation changes at high altitude with and without acetazolamide. *Invest Ophthalmol Vis Sci*. 2019;60(1):36–40.
23. Pournaras CJ, Rungger-Brändle E, Riva CE, Hardarson SH, Stefansson E. Regulation of retinal blood flow in health and disease. *Prog Retin Eye Res*. 2008;27(3):284–330.
24. Wei X, Balne PK, Meissner KE, Barathi VA, Schmetterer L, Agrawal R. Assessment of flow dynamics in retinal and choroidal microcirculation. *Surv Ophthalmol*. 2018;63(5):646–664.
25. Bosch MM, Merz TM, Barthelmes D, et al. New insights into ocular blood flow at very high altitudes. *J Appl Physiol (1985)*. 2009;106(2):454–460.
26. Hickam JB, Frayser R. Studies of the retinal circulation in man. Observations on vessel diameter, arteriovenous oxygen difference, and mean circulation time. *Circulation*. 1966;33(2):302–316.
27. Sousa DC, Leal I, Moreira S, et al. Retinal vascular reactivity in type 1 diabetes patients without retinopathy using optical coherence tomography angiography. *Invest Ophthalmol Vis Sci*. 2020;61(6):49.
28. Bhardwaj S, Tsui E, Zahid S, et al. Value of fractal analysis of optical coherence tomography angiography in various stages of diabetic retinopathy. *Retina*. 2018;38(9):1816–1823.
29. Zahid S, Dolz-Marco R, Freund KB, et al. Fractal dimensional analysis of optical coherence tomography angiography in eyes with diabetic retinopathy. *Invest Ophthalmol Vis Sci*. 2016;57(11):4940–4947.
30. Baker J, Safarzadeh MA, Incognito AV, et al. Functional optical coherence tomography at altitude: retinal microvascular perfusion and retinal thickness at 3,800 meters. *J Appl Physiol (1985)*. 2022;133(3):534–545.
31. Pechauer AD, Jia Y, Liu L, Gao SS, Jiang C, Huang D. Optical coherence tomography angiography of peripapillary retinal blood flow response to hyperoxia. *Invest Ophthalmol Vis Sci*. 2015;56(5):3287–3291.
32. Wang RK, Jacques SL, Ma Z, Hurst S, Hanson SR, Gruber A. Three dimensional optical angiography. *Opt Express*. 2007;15(7):4083–4097.
33. Kim AY, Chu Z, Shahidzadeh A, Wang RK, Puliafito CA, Kashani AH. Quantifying microvascular density and morphology in diabetic retinopathy using spectral-domain optical coherence tomography angiography. *Invest Ophthalmol Vis Sci*. 2016;57(9):Oct362–Oct370.
34. Delaey C, Van De Voorde J. Regulatory mechanisms in the retinal and choroidal circulation. *Ophthalmic Res*. 2000;32(6):249–256.
35. Lütjen-Drecoll E. Choroidal innervation in primate eyes. *Exp Eye Res*. 2006;82(3):357–361.
36. Hirano T, Chanwimol K, Weichsel J, Tepelus T, Sadda S. Distinct retinal capillary plexuses in normal eyes as observed in optical coherence tomography angiography axial profile analysis. *Sci Rep*. 2018;8(1):9380.
37. Caprara C, Grimm C. From oxygen to erythropoietin: relevance of hypoxia for retinal develop-

ment, health and disease. *Prog Retin Eye Res*. 2012;31(1):89–119.
38. Muller PJ, Deck JH. Intraocular and optic nerve sheath hemorrhage in cases of sudden intracranial hypertension. *J Neurosurg*. 1974;41(2):160–166.
39. Hayreh SS, Zimmerman MB, Podhajsky P, Alward WL. Nocturnal arterial hypotension and its role in optic nerve head and ocular ischemic disorders. *Am J Ophthalmol*. 1994;117(5):603–624.
40. Hirukawa-Nakayama K, Hirakata A, Hirakarta A, Tomita K, Hiraoka T, Inoue M. Increased choroidal thickness in patient with high-altitude retinopathy. *Indian J Ophthalmol*. 2014;62(4):506–507.
41. Sousa DC, Leal I, Moreira S, et al. A protocol to evaluate retinal vascular response using optical coherence tomography angiography. *Front Neurosci*. 2019;13:566.
42. Patton N, Aslam T, Macgillivray T, Pattie A, Deary IJ, Dhillon B. Retinal vascular image analysis as a potential screening tool for cerebrovascular disease: a rationale based on homology between cerebral and retinal microvasculatures. *J Anat*. 2005;206(4):319–348.
43. Kohner EM, Patel V, Rassam SM. Role of blood flow and impaired autoregulation in the pathogenesis of diabetic retinopathy. *Diabetes*. 1995;44(6):603–607.
44. Naeije R. Physiological adaptation of the cardiovascular system to high altitude. *Prog Cardiovasc Dis*. 2010;52(6):456–466.
45. Dünnwald T, Kienast R, Niederseer D, Burtscher M. The use of pulse oximetry in the assessment of acclimatization to high altitude. *Sensors (Basel)*. 2021;21(4):1263.
46. Seccombe LM, Peters MJ. Physiology in medicine: acute altitude exposure in patients with pulmonary and cardiovascular disease. *J Appl Physiol (1985)*. 2014;116(5):478–485.
47. Mancia G, Grassi G, Giannattasio C, Seravalle G. Sympathetic activation in the pathogenesis of hypertension and progression of organ damage. *Hypertension*. 1999;34(4 pt 2):724–728.
48. Triantafyllou A, Anyfanti P, Pyrpasopoulou A, Triantafyllou G, Aslanidis S, Douma S. Capillary rarefaction as an index for the microvascular assessment of hypertensive patients. *Curr Hypertens Rep*. 2015;17(5):33.
49. Menke MN, Dabov S, Knecht P, Sturm V. Reproducibility of retinal thickness measurements in healthy subjects using SPECTRALIS optical coherence tomography. *Am J Ophthalmol*. 2009;147(3):467–472.
50. Wolf-Schnurrbusch UE, Ceklic L, Brinkmann CK, et al. Macular thickness measurements in healthy eyes using six different optical coherence tomography instruments. *Invest Ophthalmol Vis Sci*. 2009;50(7):3432–3437.
51. Menke MN, Dabov S, Knecht P, Sturm V. Reproducibility of retinal thickness measurements in patients with age-related macular degeneration using 3D Fourier-domain optical coherence tomography (OCT) (Topcon 3D-OCT 1000). *Acta Ophthalmol*. 2011;89(4):346–351.